Advances in Technology Innovation, vol. 10, no. 3, 2025, pp. 201-219

Iterative Clipping Filtering and Saleh Model Predistorter on a MIMO-OFDM System Testbed Using Software Defined Radio

M Wisnu Gunawan, I Gede Puja Astawa*, Amang Sudarsono

Department of Electrical Engineering, Politeknik Elektronika Negeri Surabaya (PENS), Jawa Timur, Indonesia

Received 19 September 2024; received in revised form 11 January 2025; accepted 14 January 2025

DOI: https://doi.org/10.46604/aiti.2024.14310

Abstract

The purpose of this study is to address the challenges of high peak-to-average power ratio (PAPR) and nonlinear power amplifier (PA) distortion in multiple-input multiple-output orthogonal frequency division multiplexing (MIMO-OFDM) systems based on the IEEE 802.11ac. The research integrates iterative clipping filtering (ICF) for PAPR reduction and the Saleh model predistortion (PD) for PA linearization. Implemented on a software defined radio (SDR) platform using NI-USRP devices, the system is evaluated in real-world line-of-sight (LOS) and non-line-of-sight (NLOS) environments. Results show significant PAPR reduction, from 19.7 dB to 10.3 dB, and improved PA linearity, achieving a 94.80% error vector magnitude (EVM) reduction. Furthermore, the combined approach exhibits lower symbol error rates (SER) and error-free data transmission, particularly under LOS conditions. Compared to conventional methods, the system demonstrates superior execution efficiency with 475–503 ms processing times.

Keywords: iterative clipping filtering (ICF), Saleh model, multiple-input multiple-output orthogonal frequency division multiplexing (MIMO-OFDM), peak-to-average power ratio (PAPR) reduction, predistortion (PD)

1. Introduction

Orthogonal frequency division multiplexing (OFDM) has become the most dominant technology for supporting high-speed data transmission in wireless communication systems [1]. OFDM allows systems to transmit more symbols per second, thus offering high data bandwidth with high spectral efficiency suitable for application in several modern communication systems such as Digital Audio Broadcasting (DAB), Digital Video Broadcasting (DVB), wireless local area networks (WLAN), and Long Term Evolution (LTE) [2]. To further enhance channel capacity and transmission reliability, OFDM is often combined with multiple-input multiple-output (MIMO) technology, resulting in significant performance improvements in communication systems [3-4].

However, one of the main challenges faced in OFDM systems is the phenomenon of high peak-to-average power ratio (PAPR) [5-7]. This high PAPR value affects the performance of various MIMO-OFDM-based wireless communication technologies, including Wi-Fi (IEEE 802.11n), LTE, WiMAX, and the Internet of Things (IoT). In WiMAX, high PAPR makes the system highly vulnerable to the non-linearity of the power amplifier (PA), resulting in significant signal distortion and reduced transmission quality. The same issue occurs in 5G networks, where high PAPR values can reduce system performance efficiency. In the context of IoT, which often involves devices with limited resources such as battery power and processing capacity, high PAPR accelerates power consumption, thereby reducing the device's lifespan. Therefore, efficient PAPR management is crucial to maintain spectral efficiency, signal reliability, and overall system performance [8].

* Corresponding author. E-mail address: puja@pens.ac.id

Additionally, the high PAPR value forces the PA to operate in the nonlinear region, resulting in in-band distortion and interference on neighboring channels due to spectral growth [9-11]. To minimize these nonlinear effects, the PA requires operation with significant back-off, but this reduces power efficiency [12-13]. Therefore, an approach that can reduce PAPR while addressing the PA's nonlinear distortion is needed. Modern techniques such as PAPR reduction and predistortion (PD) provide important solutions to improve transmitter efficiency in wireless communication systems [14]. One simple and effective PAPR reduction technique is iterative clipping filtering (ICF), which intuitively reduces PAPR with low computational complexity [15-18]. To address the nonlinear effects of the PA, the Saleh model is used as a widely and efficiently applied behavioral model-based PD technique [19-22]. This model allows for the improvement of PA linearity by optimizing its linear operating region.

As a comparison, several studies propose an approach based on real-valued neural networks (RVNN) that integrates PAPR reduction and PD within a single framework [14]. This approach demonstrates superior performance in reducing PAPR, adjacent channel power ratio (ACPR), and bit error rate (BER). However, the RVNN-based model requires a large amount of training data and has higher computational complexity. Additionally, other research proposes a combination of PAPR reduction techniques using companding methods, such as nonlinear error function (NERF), μ-law, and hybrid, combined with Hammerstein model-based PD for OFDM systems in 5G networks [19]. This research successfully reduced the PAPR value by up to 20% and achieved a BER value of 10^{-5} at an Eb/N0 of 21 dB, demonstrating a system performance improvement of 4 dB compared to a system without PD.

However, the research did not sufficiently explore the effects of PA memory that could impact the overall system performance, including the receiver side. Therefore, the simpler ICF technique offers practical implementation advantages in hardware such as software defined radio (SDR), allowing for faster and more efficient adaptation to real-world environmental conditions. This approach not only reduces PAPR with higher computational efficiency but also provides stronger empirical validation in the context of real-world applications.

In this paper, experiments were conducted to combine PAPR reduction techniques using ICF with the Saleh model PD technique in MIMO-OFDM systems. The experiments were carried out in real time using SDR devices, specifically the USRP 2920, which allows for direct observation of the algorithm's effectiveness under real operational conditions [23-24]. The testing involves the transmission of text data to evaluate the performance of PAPR reduction techniques using complementary cumulative distribution function (CCDF), PD with AM/AM, and power spectral density (PSD) graphs, as well as the overall system performance through constellation diagrams, error characteristics, and symbol error rate (SER) analysis on the receiver side [25]. This research is expected to provide stronger empirical insights and validation for the application of ICF techniques and the Saleh model in real-world MIMO-OFDM systems.

2. System Modelling

This section covers the architecture of the MIMO-OFDM system at both the transmitter and receiver ends, the parameters used in the OFDM system, the mathematical representation of the Saleh model, and the iterative ICF process, providing a comprehensive framework for understanding and applying these techniques in modern wireless communication systems.

2.1. MIMO-OFDM design

In implementing the MIMO-OFDM system with the application of ICF and the Saleh model based on SDR, on the transmitter side, a PC running LabVIEW controls USRP 1 and USRP 2 to generate and transmit OFDM data via antenna, using PA to amplify Radio Frequency (RF) data. The MIMO channel then transfers the signal. Subsequently, USRP 3 and USRP 4 transform the RF created by the PA into a digital signal for longer-term analysis on a PC, as shown in Fig. 1.

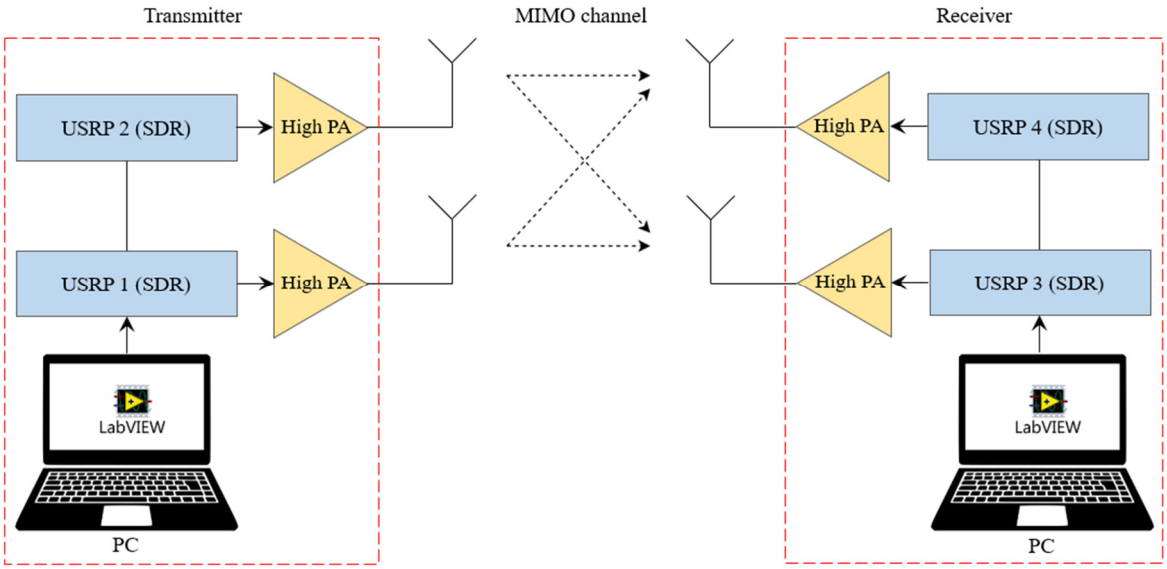

Fig. 1 Designing a hardware implementation of MIMO-OFDM system

The purpose of this system is to monitor MIMO-OFDM communication performance, including SER analysis, PAPR implementation, and PA segmentation. Table 1 clearly explains the OFDM parameter used in the implementation of the SDR-based system. OFDM settings in Table 1 are updated per IEEE 802.11ac.

Table 1 OFDM parameters

Parameter	Value
FFT size	128
Number of subcarriers	128
Number of data subcarriers	96
Number of pilot subcarriers	8
Number of null subcarriers	24
Modulation	4-QAM
Cyclic prefix	32
Center frequency	915 Hz
Channel estimation	Least square
Channel equalizer	Zero forcing

Recent Wi-Fi standards like IEEE 802.11ac offer high data transmission speeds, massive network capacity, and excellent spectrum efficiency. The OFDM configuration of this standard uses 128 subcarriers, 96 of which are used for data transmission and the rest for zero padding and pilot symbols. Data subcarriers are the main medium for user data transport, enabling fast speeds. Pilot subcarriers reference phase and frequency adjustment during transmission, ensuring signal reliability, especially in dynamic communication channels. Certain subcarriers have zero padding to reduce inter-channel interference and ensure fast Fourier transform (FFT) size compatibility. IEEE 802.11ac uses Quadrature Amplitude Modulation (QAM) modulation to optimize spectral efficiency. This standard meets modern networks' high-speed, high-capacity data transmission needs with this design and QAM modulation.

The transmitter and receiver processes are depicted in Fig. 2 and Fig. 3, respectively. On the transmitter side, text data is first converted into a bit sequence mapped to QAM constellation symbols. The symbols, totaling n = 2 N (where N = 96), are split into two sequences of n/2 symbols each. These sequences are converted from serial to parallel format, with 24 null symbols and nine pilot symbols added, resulting in parallel sequences of length 128. Afterward, the inverse fast Fourier transform (IFFT) process transforms these into time-domain symbols, followed by PAPR reduction using the ICF technique. A cyclic prefix is added to mitigate interference, and PD based on the Saleh model is applied before the internal PA of the USRP amplifies the signal. The cyclic prefix is removed at the receiver, and FFT converts the received signal into frequency-

domain symbols. Channel estimation, equalization, and removing pilot and null symbols are performed, followed by parallel-to-serial conversion. The MIMO-OFDM decoder combines the outputs from the receiving antennas, producing a single QAM symbol sequence, which is remapped into bits and converted back to text.

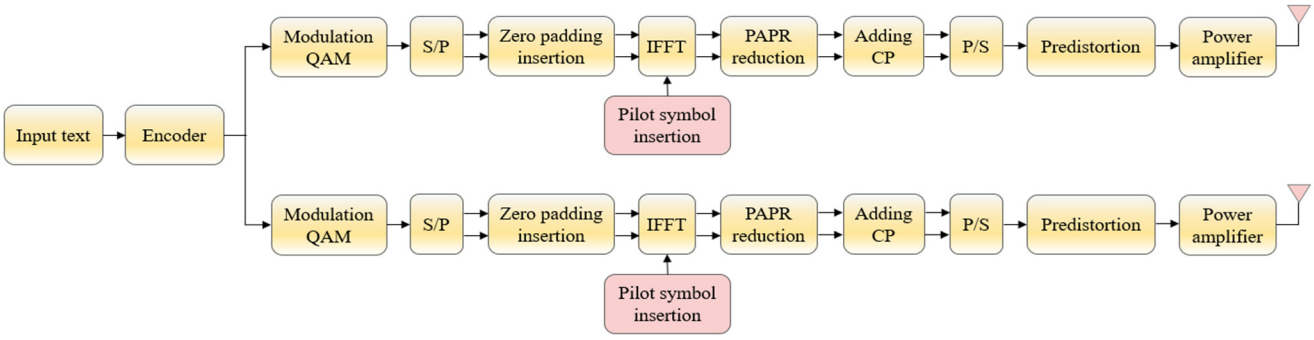

Fig. 2 Block diagram of MIMO-OFDM transmitter system

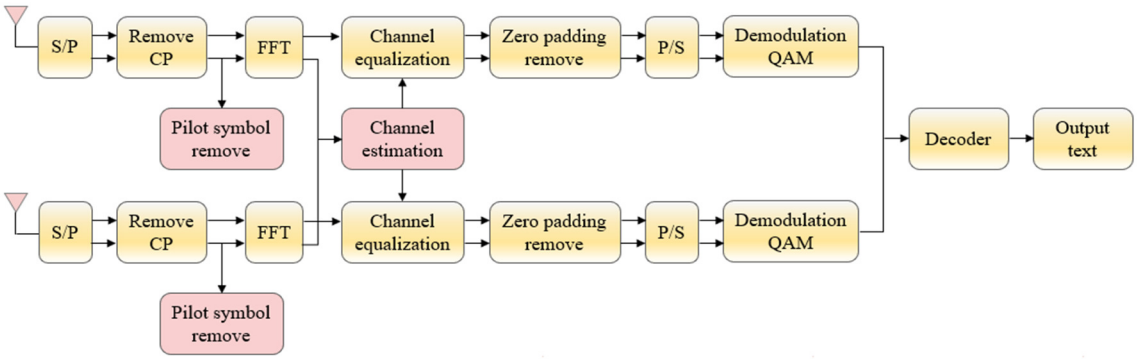

Fig. 3 Block diagram of MIMO-OFDM receiver system

2.2. *ICF for PAPR reduction*

In an OFDM system, the OFDM signal consists of the summation of several independently modulated subcarriers. If the phase of each subcarrier is the same, the maximum signal power generated will be N times its average power. The ratio between the maximum signal power and the average power is commonly referred to as the PAPR. At any given time, this summation can be very large and, at other times, very small, meaning that the maximum power value of the signal is always greater than its average power. Mathematically, the PAPR of a signal is defined by the formula below.

$$PAPR = \frac{P_{peak}}{P_{average}} = \frac{\max |x(n)|^2}{E\left(|x(n)|^2\right)} \tag{1}$$

where P_{peak} denotes the maximum power (watts) and $P_{average}$ average power (watts). The term $max|x(n)|^2$ represents the peak value of the OFDM signal while $E(|x(n)|^2)$ the average value of the OFDM signal. The PAPR value from Eq. (1) can be converted to dB using the formula below.

$$PAPR(dB) = 10\log_{10}(\text{PAPR}) \tag{2}$$

The PAPR value is generally statistically described using the CCDF. The CCDF is used to analyze and compare PAPR values. The CCDF is expressed as follows.

$$CCDF = 1 - CDF \tag{3}$$

$$CCDF = 1 - \left(1 - e^{-PAPR}\right)N \tag{4}$$

Eq. (4), the input values are the PAPR and N, representing the number of subcarriers used in the OFDM system.

A high PAPR value in OFDM requires an amplifier with a wide dynamic range to accommodate the signal amplitude. If this is not met, it will cause linear distortion, resulting in the subcarriers losing their orthogonality and ultimately degrading the performance of the OFDM system. This high PAPR issue cannot be ignored, as it can reduce the performance of the OFDM communication system. Therefore, techniques to reduce high PAPR values are necessary. Conceptually, PAPR reduction techniques aim to reduce the OFDM signal's peak power or average power. By reducing the peak power or average power, the requirement for input back-off (IBO) can be minimized, thereby improving the performance of the OFDM system. Commonly used techniques to reduce PAPR include partial transmit sequence (PTS), clipping filtering (CF), and ICF, which rely on an adjustable clipping ratio (CR) parameter. A comparison of ICF with other PAPR reduction algorithms is shown in Table 2.

Table 2 Comparison of ICF with other PAPR reduction algorithms

Criteria	ICF	PTS
Computational complexity	Low (simple to implement)	High (requires phase optimization for each subblock)
Effectiveness of PAPR reduction	Effective at certain CR values	More effective with proper optimization
Signal distortion	Potentially introduces distortion	Does not cause distortion
Implementation flexibility	Easy to implement on SDR devices	Requires phase optimization algorithms
Parameter sensitivity	Highly dependent on CR value	Dependent on the number of subblocks
Advantages	Easy to implement and efficient	Provides optimal minimum PAPR results
Disadvantages	Signal distortion due to the clipping process	High computational complexity

ICF is a PAPR reduction method that enhances the CF method. ICF works similarly to CF, but it involves iterations during the clipping and filtering process. The ICF method directly reduces the signal peaks using a predetermined threshold. Then, the clipped signal is filtered to eliminate out-of-band (OOB) radiations that occur due to the clipping process. Iteration in this method is performed to address peak regrowth, which usually occurs after the filtering process. Additionally, iteration is used to achieve the targeted PAPR value. The ICF method can be defined using:

$$\hat{x}(n)=\begin{cases} A_{\max}e^{j\varphi t} & \left|x^{i}(n)\right|>A_{\max} \\ x^{i}(n), & \left|x^{i}(n)\right|\le A_{\max} \end{cases} \tag{5}$$

2.3. *Saleh model predistortion*

A PA is a nonlinear component of the system. Ideally, the output of the PA is equivalent to the input multiplied by a gain factor. The PA has a limited linear region beyond which it reaches saturation at the maximum output level, as illustrated in Fig. 4.

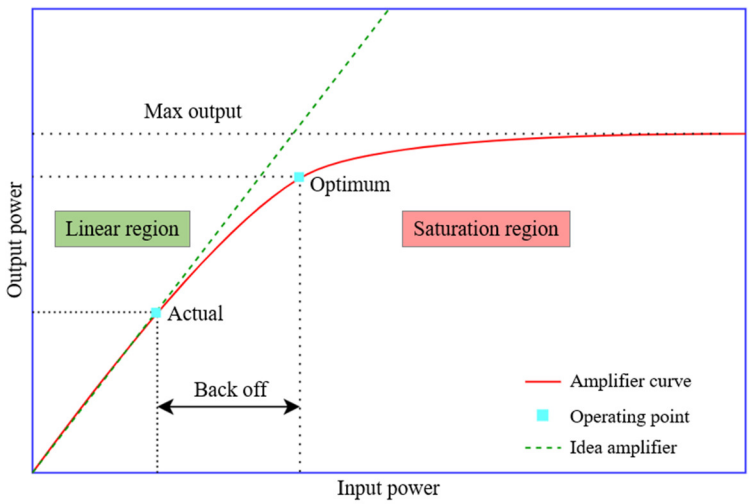

Fig. 4 Power amplifier operating region curve

PA exhibits nonlinear characteristics, saturation happens when the input signal surpasses a particular level. A signal with a high PAPR passing via a PA may cause saturation. Saturation distorts the input signal since the PA no longer performs linearly at high power. This distortion occurs inside and outside the frequency band. In-band distortion lowers the signal quality and increases the BER. Spectrum efficiency is reduced by OOB distortion, which interferes with nearby channels. This nonlinear distortion affects MIMO-OFDM and other RF signal transmission technologies like 5G, IoT, and others. Nonlinear distortion in many communication systems, especially those that deliver data quickly or have limited resources, must be managed to minimize spectrum and power utilization. To handle PA nonlinearity, a linearization method is needed. Modeling the PA to understand its linearization model achieves linearization. Use the Saleh model to model the PA.

The Saleh model models nonlinear PA. This memoryless model shows that PA characteristics don't change and are easy to implement. Although rapid for calculations, the Saleh model cannot imitate the nonlinear behavior of current amplifiers, especially solid-state amplifiers. This model misrepresents power compression and phase distortion at sub-THz frequencies, especially under saturation. This model also struggles with high-frequency amplifiers complex intermodulation and even-order nonlinearities. The model's fundamental structure is easy to build, but its limits make it ideal for low-frequency and non-saturation applications. Complex applications require parametric modifications or neural network-based methods to define modern PA nonlinear properties. Table 3 contrasts the Saleh model with various PD models. The PA model can be expressed as follows:

$$y(u) = \frac{\alpha u^{\eta}}{\left(1+\beta u^{2}\right)^{v}} \tag{6}$$

The output signal of the PA is denoted as $y(u)$, which is a function of the input signal to the PA, u. The PA coefficients, obtained from measurements, are represented as α and β. Additionally, there are preselected parameters, which can take values of 1, 2, or 3, and which can take values of 1 or 2.

Table 3 Comparison of the Saleh model with other predistortion models

Criteria	Saleh model	Neural network
Computational complexity	Low (analytical and straightforward)	High (requires training and inference processes)
Effectiveness in linearization	Effective for low-to-moderate nonlinearities	Highly effective, adaptable to complex nonlinearities
Flexibility	Limited (specific to certain amplifier types)	High (applicable to various nonlinear systems)
Adaptability	Low (fixed parameters)	High (self-learning capability allows adaptation)
Accuracy in nonlinear modeling	Moderate (simplified nonlinear model)	High (captures complex nonlinearities)
Advantages	Simple, low computation, suitable for real-time	Can handle highly complex systems and dynamics
Disadvantages	Limited to specific amplifier characteristics	Computationally intensive and requires significant data for training

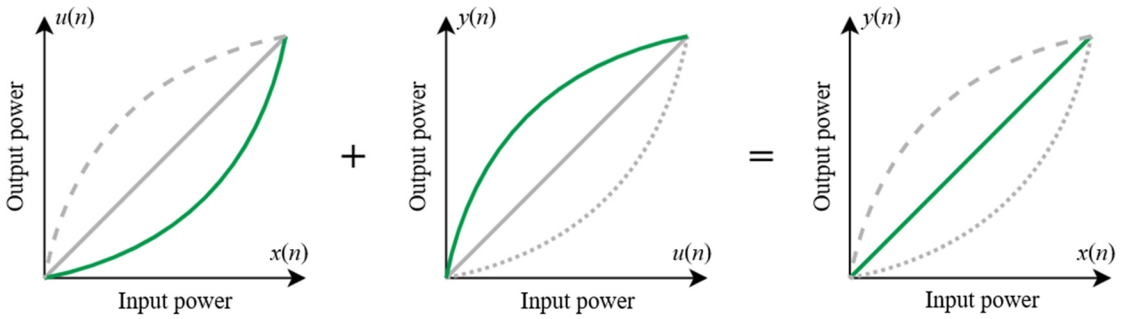

Fig. 5 Transfer function of the combined PA-PD

PD is a technique used to linearize PA. The PD model characterizes the inverse behavior of the PA. As shown in the transfer function diagram in Fig. 5, when PD is combined with the PA, it results in a linear system. When PD is applied alongside the PA, it compensates for the amplifier's nonlinear behavior, effectively transforming the overall system into a linear one.

Thus, it is understood that the input signal $x(n)$ first passes through a predistorter, which has a model characteristic that is the inverse function of the PA's transfer function. The output of the PD is then used as input for the PA. The PD equation is given as follows.

$$u(x) = H^{-1}\left[y(x)\right] \tag{7}$$

The output signal of the predistorter is denoted by $u(x)$, which is obtained from the inverse of the equation $y(x)$. The inverse function for PD is given by H^{-1}.

Therefore, the inverse function for the polar parameter AM/AM in the Saleh model PD is provided as follows.

$$H^{-1}(x) = \frac{\alpha - \sqrt{\alpha^2 - 4\beta x^2}}{2\beta x} \tag{8}$$

In Eq. (8), α and β are constants derived from the characteristics of the PA, and x is the input value to the inverse function. The term under the square root, $a^2 - 4\beta x^2$, is the discriminant of the quadratic equation, which influences the shape of the curve in the original PA model. This inverse function is used to linearize the PA by ensuring that the output signal, after PD when passed through the PA, results in a linear response.

3. Results and Discussion

This section analyzes the performance of various techniques implemented in the MIMO-OFDM system. The discussion covers the evaluation of the ICF technique for PAPR reduction, the effectiveness of the Saleh model-based PD technique in linearizing PA, and the application of this approach within the MIMO-OFDM framework. Furthermore, it examines the combined use of the Saleh model PD technique and ICF in the MIMO-OFDM system and analyzes the relationship between SER and signal-to-noise ratio (SNR). The evaluation results highlight the system's effectiveness in enhancing signal transmission quality.

3.1. Performance ICF for PAPR reduction

The CCDF curve in Fig. 6 represents the probability of PAPR values for signals generated from a MIMO-OFDM system that implements PAPR reduction techniques using ICF with various CR values and a system that does not apply PAPR reduction techniques. $PAPR_0$ indicates the power level generated based on the range of PAPR values for each generated symbol. The CCDF curve shown in Fig. 6 provides the PAPR values achieved using the ICF technique for PAPR reduction. These values correspond to the most negligible probabilities observed in the simulation, highlighting the effectiveness of the ICF method in minimizing PAPR under specific conditions.

Table 4 PAPR values of MIMO-OFDM system with and without ICF

System scenario	PAPR value
OFDM	19.7 dB
OFDM + ICF CR = 5	12.1 dB
OFDM + ICF CR = 4	11.3 dB
OFDM + ICF CR = 3	10.3 dB

The detailed numerical results from the CCDF curve are summarized and presented comprehensively in Table 4 for further analysis and comparison. The results show that the OFDM signal with the PAPR reduction technique using ICF has a lower power level than the OFDM signal without the PAPR reduction technique. The CR value affects the extent of the CR to reduce the PAPR value. A smaller CR value results in a lower power level.

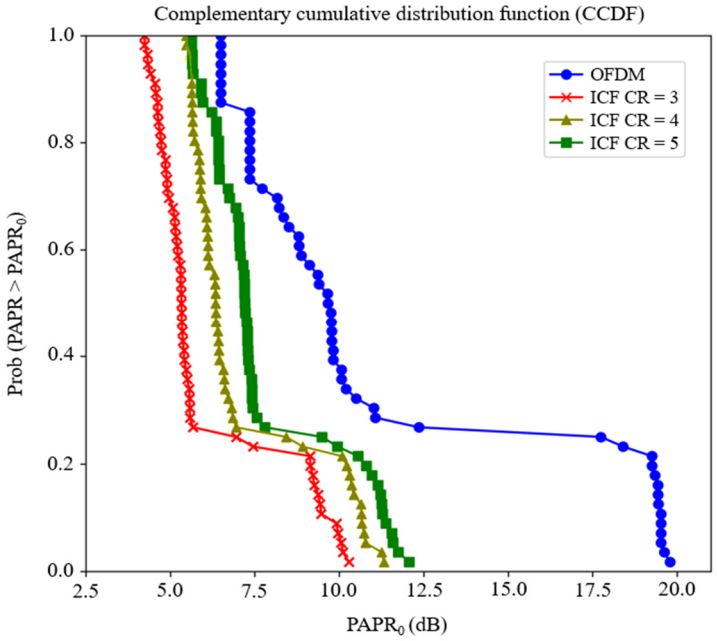

Fig. 6 CCDF curves of the MIMO-OFDM system without and with ICF

ICF is used with confidence interval (CI) analysis to evaluate PAPR reduction efficiency. PAPR reduction CIs for various CRs are presented in Fig. 7. In Fig. 7, three graphs show PAPR reduction performance (in dB) for the reduction technique with CR values of 3, 4, and 5. In the graph for CR = 3, PAPR reduction averages 6.33 dB with a 95% CI of [5.38, 7.28]. It reduces PAPR significantly, but sample variance is substantial, especially after the 30th sample, indicating uneven signal clipping. Graph for CR = 4 indicates an average PAPR reduction of 5.26 dB with a 95% CI [4.32, 6.19]. This number balances PAPR reduction performance and result consistency, with lower sample variation than CR = 3.

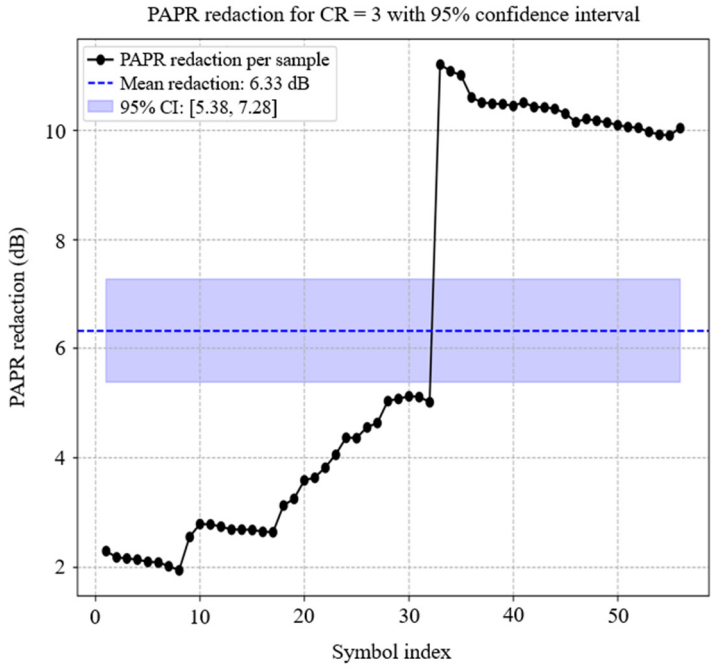

(a) CR = 3

Fig. 7 Confidence interval for several CR values

In the graph for CR = 5, the average PAPR reduction is 4.51 dB with a 95% CI of [3.61, 5.41]. Better stability is observed at CR = 5, as indicated by the lower sample variance. The lower PAPR reduction suggests that higher CRs produce more stable signals but achieve less PAPR reduction. Overall, the results indicate that the CR value should balance PAPR reduction and signal stability, depending on application needs.

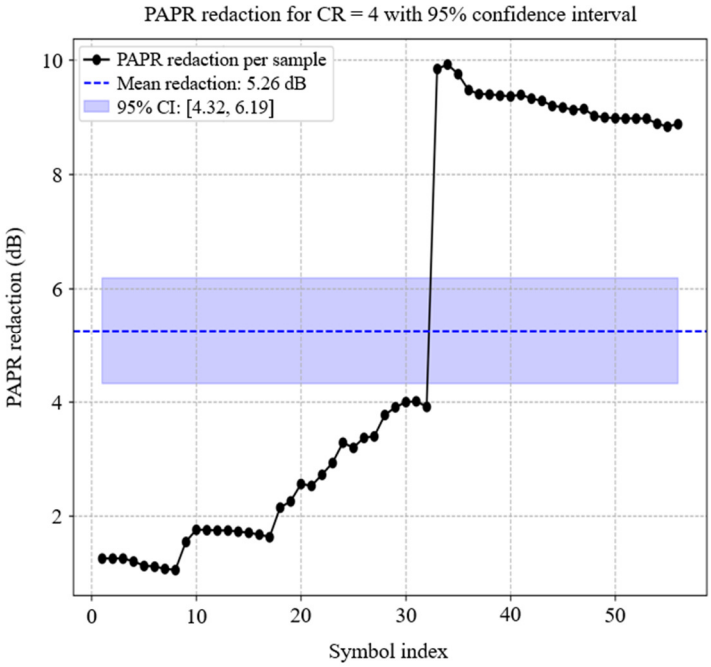

(b) CR = 4

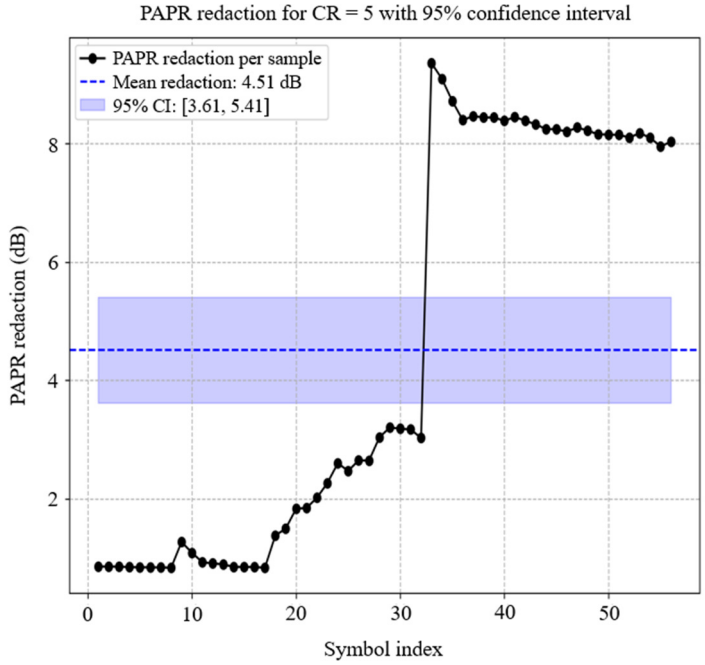

(c) CR = 5

Fig. 7 Confidence interval for several CR values (continued)

Based on the execution time data in Table 5, ICF is far more efficient than PTS in terms of execution time. ICF only requires 3–8 ms for all values of CR, indicating that this algorithm is very simple and suitable for real-time applications that prioritize time efficiency. In contrast, PTS takes much longer, at 293 ms, because the process involves dividing the OFDM signal into sub-blocks, searching for the optimal phase, and reassembling, thereby increasing computational complexity. Therefore, PTS is more suitable for applications that prioritize optimal PAPR reduction, while ICF excels in time efficiency for signal processing.

Table 5 Comparison of execution time for several scenarios

Scenario	Execution time
MIMO-OFDM + PA-PD ICF CR = 3	503 ms
MIMO-OFDM + PA-PD ICF CR = 4	483 ms
MIMO-OFDM + PA-PD ICF CR = 5	475 ms
MIMO-OFDM + PAPR reduction PTS	776 ms
PAPR reduction ICF CR = 3	8 ms
PAPR reduction ICF CR = 4	4 ms
PAPR reduction ICF CR = 5	3 ms
PAPR reduction PTS	293 ms

3.2. Performance Saleh model PD technique for PA linearization

The AM/AM curves of the PD output signal, PA output signal, and combined PA-PD output signal are shown in Fig. 8. The AM/AM curves show that the PA output signal Fig. 8(b) is nonlinear, supporting the idea that PAs are signal amplifying components. The AM/AM curve for the PD output signal Fig. 8(a) is the opposite of the PA output signal Fig. 8(b). As demonstrated in Fig. 8(c), the AM/AM curve is linear when the PD and PA output signals are combined. This shows that linearizing the nonlinear PA in the Saleh model PD extends the back-off region.

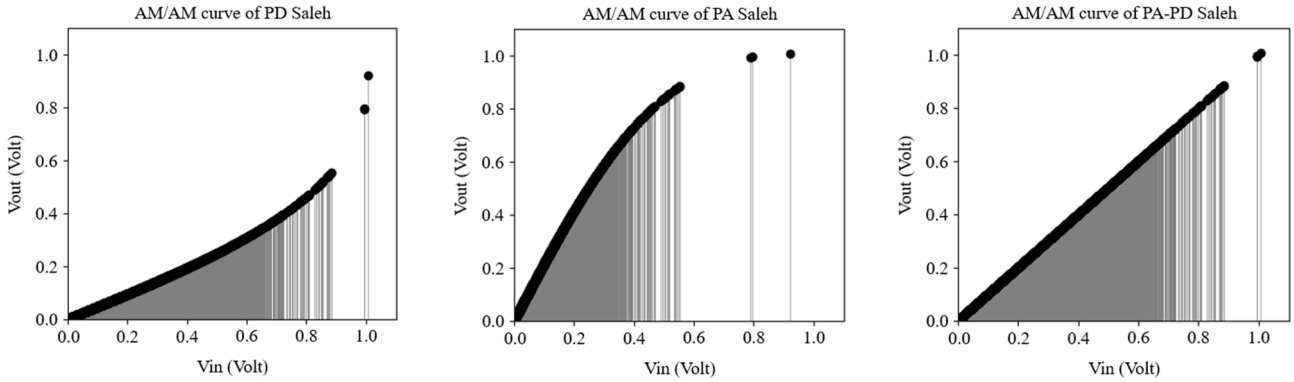

(a) AM/AM PD curve (b) AM/AM PA curve (c) AM/AM Linear PA-PD curve

Fig. 8 AM/AM curve of linearization PA

In addition to using AM/AM curves, the impact of the Saleh model PD in linearizing the nonlinear PA is also demonstrated using PSD plots, as shown in Fig. 9. The PSD graph reveals the influence of the PA's nonlinear characteristics on OOB emissions, resulting in additional spectral components outside the desired frequency band. By applying PD, the nonlinear effects of the PA that cause OOB emissions can be compensated.

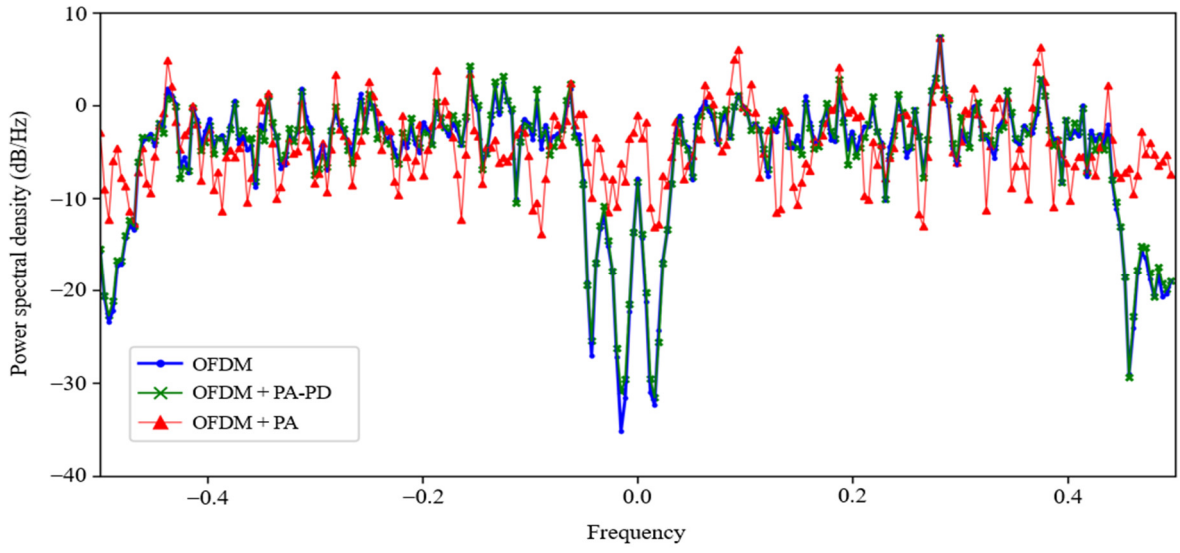

Fig. 9 PSD graph of MIMO-OFDM system with linearization PA

The application of PD techniques significantly improves the linearity of the PA, with error vector magnitude (EVM) reduced from 62.11% to 3.23%, reflecting an improvement of 94.80%, as shown in Fig. 10. This reduction in EVM indicates that PD is effective in reducing nonlinear distortion, enhancing signal quality, and ensuring transmission reliability in wireless communication systems.

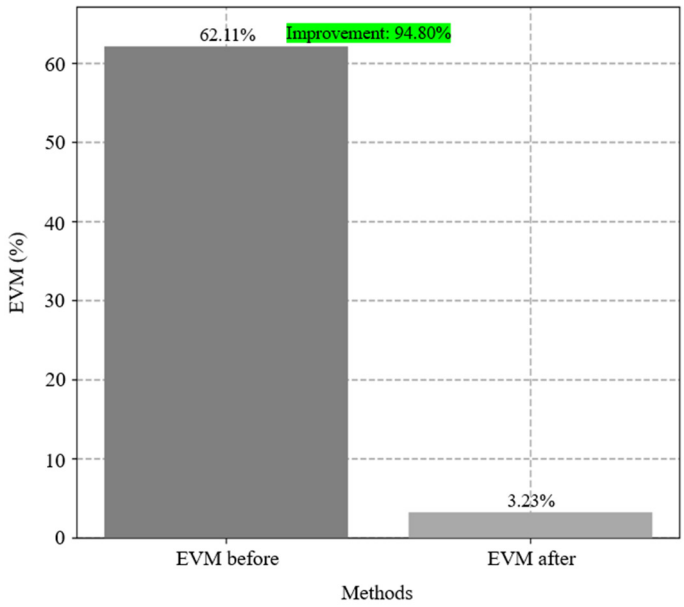

Fig. 10 Comparison before and after predistortion

3.3. Performance of the Saleh model PD technique in MIMO-OFDM systems

Fig. 11 System testing on LOS condition

Fig. 12 System testing on NLOS condition

The Saleh model PD technique was tested in MIMO-OFDM systems under line-of-sight (LOS) and non-line-of-sight (NLOS) situations, as shown in Fig. 11 and Fig. 12. Testing took place at the postgraduate building, PENS, an interior environment with several actual constraints that could impair communication system performance. People walking by, using electronics, and architectural components like walls, floors, and ceilings reflecting signals make this setting noisy. Mobile phone and Wi-Fi router interference can further degrade the system. This real-world scenario necessitates a reliable and optimal system amid dynamic and disruptive operations.

Each transmitter and receiver is configured using the SDR device according to the settings shown in Fig. 13. SDR provides advantages in terms of hardware control through software, allowing experiments with various PAPR reduction techniques, testing of various signal parameters, and evaluation of communication system performance under varying conditions. The SDR device used is the NI-USRP 2920, which supports the MIMO scheme.

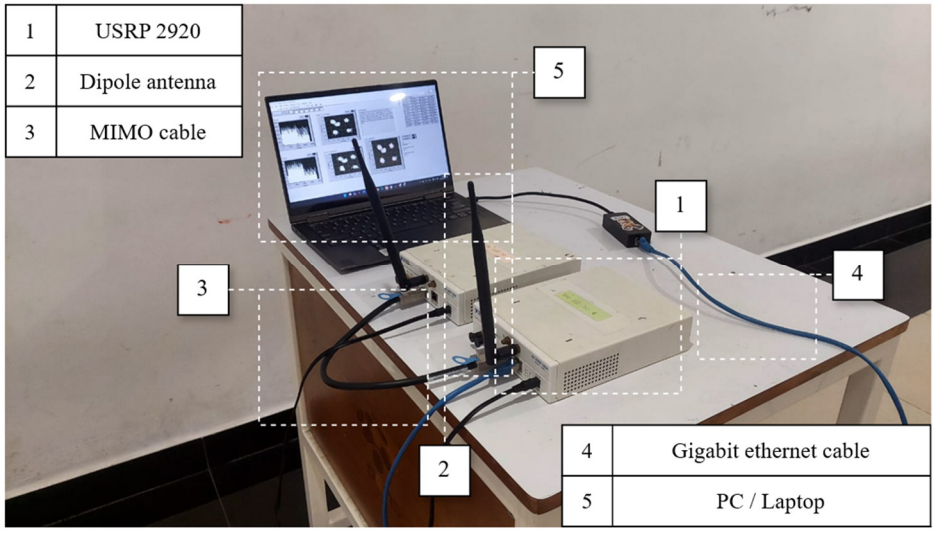

Fig. 13 Configuration of SDR device

The NI-USRP device is used to transmit and receive RF signals. Each NI-USRP device has an antenna that allows for the transmission and reception of wireless signals. Since the testing uses a 2×2 MIMO scheme, two NI-USRP devices are used as transmitters, and two other devices are used as receivers. MIMO cable synchronizes both NI-USRP devices configured as transmitters or receivers. Therefore, the MIMO cable guarantees that no processes take precedence over each other during the MIMO process. LabVIEW software controls and configures the NI-USRP devices as transmitters and receivers on a PC or laptop.

Testing was conducted by transmitting text from the transmitter to the receiver. The text sent is shown in Fig. 14. The testing was performed by analyzing the output constellation diagram and the number of character errors. The first test involved a MIMO-OFDM system using a PA without PD. Subsequently, the MIMO-OFDM system was tested using a PA with the Saleh model PD technique application.

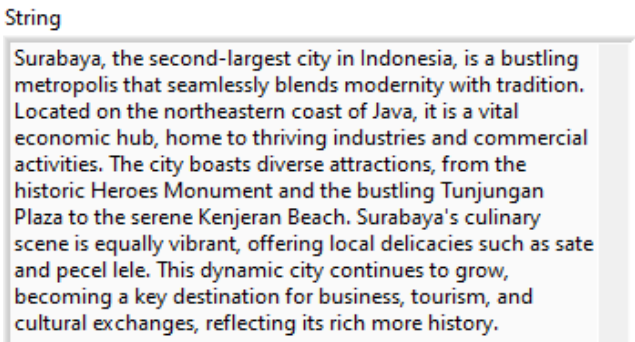

Fig. 14 Data text source

The constellation diagram still matches the 4-QAM modulation in the findings of the PA-only system test. However, many constellation symbols are incorrect. Because of the nonlinearity of PA, the received symbols still contain errors. The incorrect symbols are translated into text using a constellation diagram with error symbols. As shown in Table 6, the LOS scenario receives one incorrect character, while the NLOS scenario in Table 7, receives eight incorrect characters. The constellation diagram for the PA system using the Saleh model PD technique shows 4-QAM modulation with non-dispersed symbols. The Saleh model PD technique improves system performance by eliminating receiver character errors.

Table 6 Constellation and character results of MIMO-OFDM under LOS conditions with and without PD

Scenario	Constellation diagram	Display character error
MIMO-OFDM system using PA	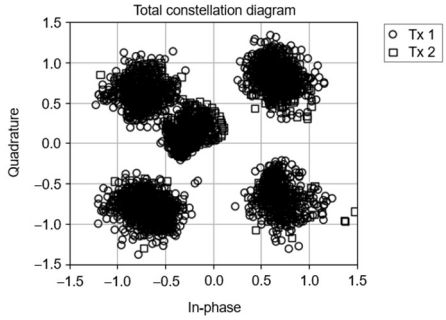	string 2 Surabaya, the second-largest city in Indonesia, is a bustling metropolis that seamlessly blends modernity with tradition. Located on the northeastern coast of Java, it is a vital economic hub, home to thriving industries and commercial activities. The city boasts diverse attractions, from the historic Heroes Monument and the bustling Tunjungan Plaza to the serene Kenjeran Beach. Surabaya's culinary scene is equally vibrant, offering local delicacies such as sate and pecel lele. This dynamic city continues to grow, becoming a key destination for business, tourism, and culturàl exchanges, reflecting its rich more history.
MIMO-OFDM system using PA with PD	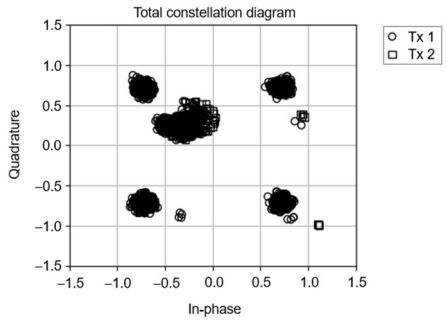	string 2 Surabaya, the second-largest city in Indonesia, is a bustling metropolis that seamlessly blends modernity with tradition. Located on the northeastern coast of Java, it is a vital economic hub, home to thriving industries and commercial activities. The city boasts diverse attractions, from the historic Heroes Monument and the bustling Tunjungan Plaza to the serene Kenjeran Beach. Surabaya's culinary scene is equally vibrant, offering local delicacies such as sate and pecel lele. This dynamic city continues to grow, becoming a key destination for business, tourism, and cultural exchanges, reflecting its rich more history.

Table 7 Constellation and character results of MIMO-OFDM under NLOS conditions with and without PD

Scenario	Constellation diagram	Display character error
MIMO-OFDM system using PA	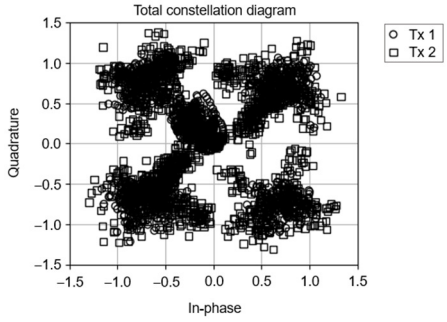	string 2 Surabaya, the second-largest city in Indonesia, is a bõstling metropolis that seamLessly blends modernity with traditioN. Located on the northeastern coast of Java, it is a vital economic hub, home to thriving industries and commercial activities. The city boasts diverse attractions, from the historic Heroes Monument and the justlinG Tunjungan Plaza to the serene Kenjeran Beach. Surabaya's culinary scene is equally vibrant, mffering local delicacies such as sate and pecel lele. This dynamic city continues to grow, becoming a key destination for business, tourism, and culturàl exchanges, reflecting its rich more history.
MIMO-OFDM system using PA with PD	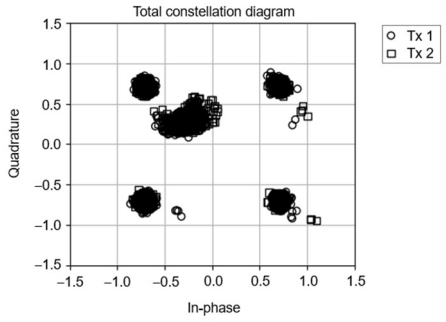	string 2 Surabaya, the second-largest city in Indonesia, is a bustling metropolis that seamlessly blends modernity with tradition. Located on the northeastern coast of Java, it is a vital economic hub, home to thriving industries and commercial activities. The city boasts diverse attractions, from the historic Heroes Monument and the bustling Tunjungan Plaza to the serene Kenjeran Beach. Surabaya's culinary scene is equally vibrant, offering local delicacies such as sate and pecel lele. This dynamic city continues to grow, becoming a key destination for business, tourism, and cultural exchanges, reflecting its rich more history.

3.4. Performance of the Saleh model PD technique and PAPR reduction using ICF in MIMO-OFDM systems

The effects of PAPR reduction techniques and PD can be analyzed through the transmitted signals from the transmitter. This Fig. 15 shows what happened to the signals sent from the transmitter when the ICF method was used with CR values of

3, 4, and 5. From Fig. 15, it can be observed that the signals transmitted by the MIMO-OFDM system with the implementation of the ICF method and the Saleh model PD experience a decrease in amplitude value. This is attributed to the influence of ICF in clipping the transmitted signals.

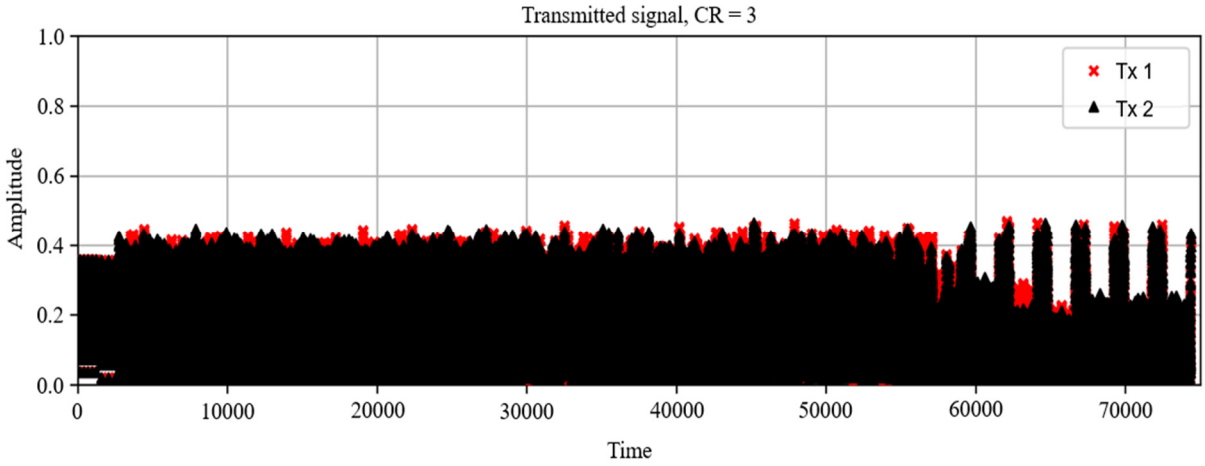

(a) CR = 3

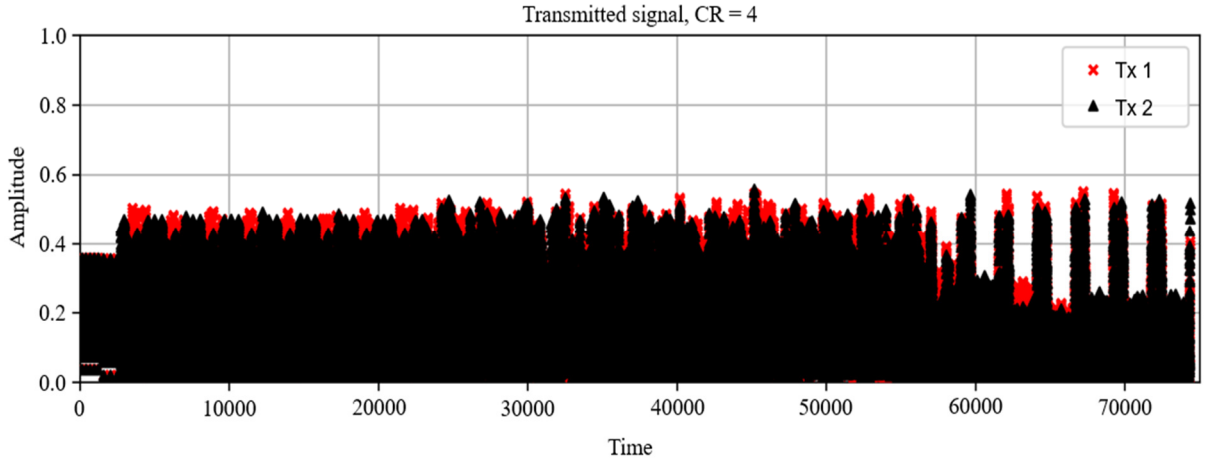

(b) CR = 4

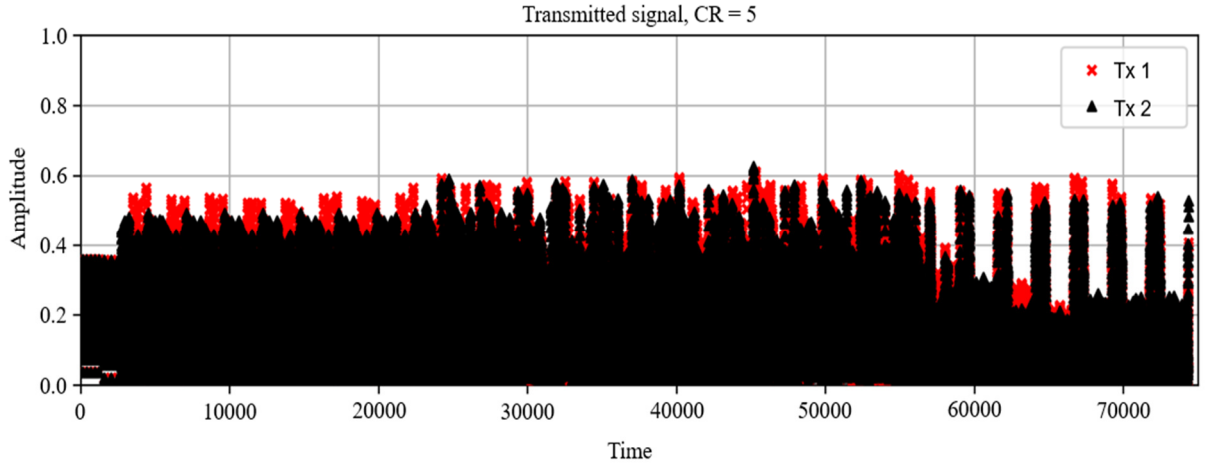

(c) CR = 5

Fig. 15 The transmitted signal for various CR parameters

From each configuration of CR values, tests will be conducted to evaluate the transmission performance of the MIMO-OFDM system by applying the ICF technique and Saleh's model PD through the observation of character errors and constellation diagrams under LOS and NLOS conditions. The characters and constellation diagrams received under LOS conditions for CR values of 3, 4, and 5 are displayed in Table 8.

Table 8 Constellation and character results of MIMO-OFDM with PD and PAPR reduction at various CRs under LOS conditions

Scenario	Constellation diagram	Display character error
MIMO-OFDM system using PD and ICF CR = 3	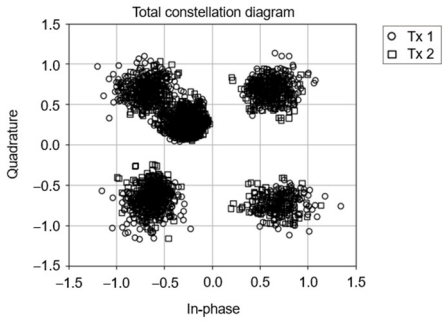	string 2 Surabaya, the second-largest city in Indonesia, is a bustling metropolis that seamlessly blends modernity with tradition. Located on the northeastern coast of Java, it is a vital economic hub, home to thriving industries and commercial activities. The city boasts diverse attractions, from the historic Heroes Monument and the bustling Tunjungan Plaza to the serene Kenjeran Beach. Surabaya's culinary scene is equally vibrant, offering local delicacies such as sate and pecel lele. This dynamic city continues to grow, becoming a key destination for business, tourism, and cultural exchanges, reflecting its rich more history.
MIMO-OFDM system using PD and ICF CR = 4	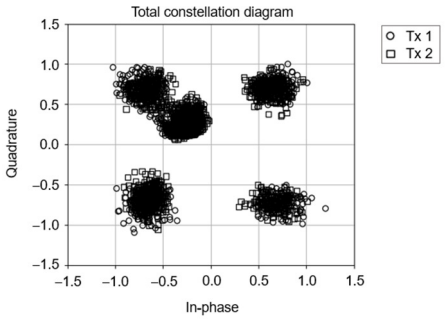	string 2 Surabaya, the second-largest city in Indonesia, is a bustling metropolis that seamlessly blends modernity with tradition. Located on the northeastern coast of Java, it is a vital economic hub, home to thriving industries and commercial activities. The city boasts diverse attractions, from the historic Heroes Monument and the bustling Tunjungan Plaza to the serene Kenjeran Beach. Surabaya's culinary scene is equally vibrant, offering local delicacies such as sate and pecel lele. This dynamic city continues to grow, becoming a key destination for business, tourism, and cultural exchanges, reflecting its rich more history.
MIMO-OFDM system using PD and ICF CR = 5	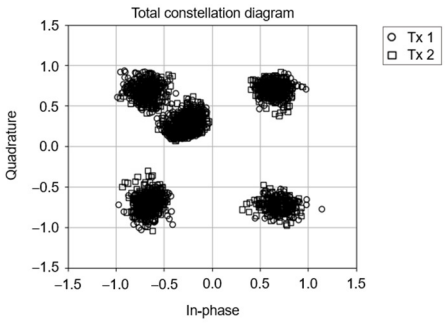	string 2 Surabaya, the second-largest city in Indonesia, is a bustling metropolis that seamlessly blends modernity with tradition. Located on the northeastern coast of Java, it is a vital economic hub, home to thriving industries and commercial activities. The city boasts diverse attractions, from the historic Heroes Monument and the bustling Tunjungan Plaza to the serene Kenjeran Beach. Surabaya's culinary scene is equally vibrant, offering local delicacies such as sate and pecel lele. This dynamic city continues to grow, becoming a key destination for business, tourism, and cultural exchanges, reflecting its rich more history.

Table 9 Constellation and character results of MIMO-OFDM with PD and PAPR reduction at various CRs under NLOS conditions

Scenario	Constellation diagram	Display character error
MIMO-OFDM system using PD and ICF CR = 3	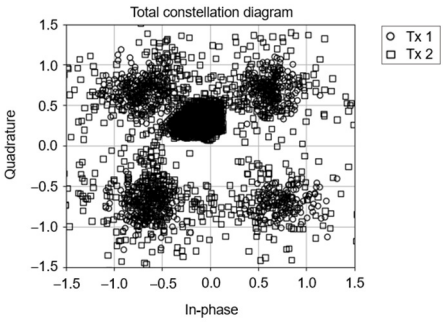	string 2 Surabaya, the second-largest city in Indonesia, is a bŏstling metropolis that seamLessly blends modernity with traditioN. Located on the northeastern coast of Java, it is a vital economic hub, home to thriving industries and commercial activities. The city boasts diverse attractions, from the historic Heroes Monument and the justlinG Tunjungan Plaza to the serene Kenjeran Beach. Surabaya's culinary scene is equally vibrant, offering local delicacies such as sate and pecel Lele. This dynamic city continues to grow, becoming a key destination for business, tourism, and culturàl exchanges, reflecting its rich more history.
MIMO-OFDM system using PD and ICF CR = 4	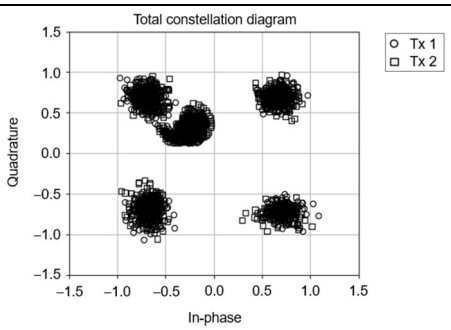	string 2 Surabaya, the second-largest city in Indonesia, is a bustling metropolis that seamlessly blends modernity with tradition. Located on the northeastern coast of Java, it is a vital economic hub, home to thriving industries and commercial activities. The city boasts diverse attractions, from the historic Heroes Monument and the bustling Tunjungan Plaza to the serene Kenjeran Beach. Surabaya's culinary scene is equally vibrant, offering local delicacies such as sate and pecel lele. This dynamic city continues to grow, becoming a key destination for business, tourism, and cultural exchanges, reflecting its rich more history.

Table 9 Constellation and character results of MIMO-OFDM with PD and PAPR reduction at various CRs under NLOS conditions (continued)

Scenario	Constellation diagram	Display character error
MIMO-OFDM system using PD and ICF CR = 5	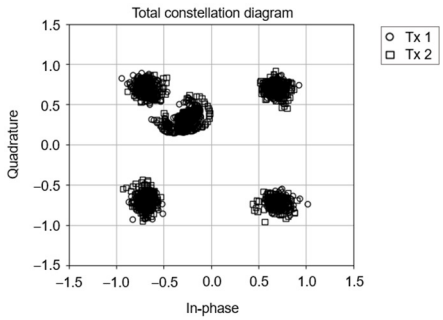	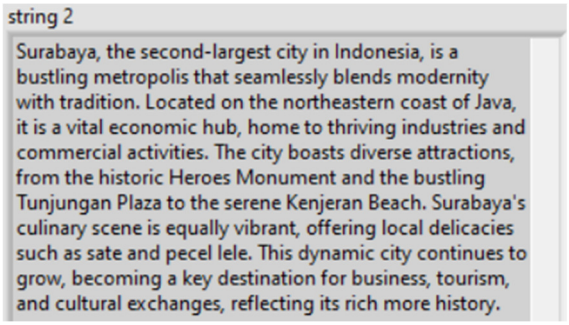

The characters and constellation diagrams received under NLOS conditions for CR values of 3, 4, and 5 are displayed in Table 9. For LOS and NLOS conditions, when the CR value is 3, there are character errors compared to the results from CR values of 4 and 5. Additionally, the constellation diagram at a CR value of 3 also shows greater dispersion. Character errors and dispersion in the constellation diagram are caused by the smaller CR value, which results in a lower signal level, thereby degrading transmission efficiency. This is a weakness of the ICF algorithm, so determining the optimal CR value should not only focus on reducing PAPR but also consider overall transmission performance.

3.5. Evaluation of SER against transmission distance

The curves in Fig. 16 and Fig. 17 show the relationship between transmission distance and the reliability of the communication system, where distance is used as a substitute for the SNR value. The assumption is that the smaller the distance between the transmitter and receiver, the stronger the signal will be, resulting in a higher SNR and a lower SER. The distance settings in the tests were conducted at 120, 180, 240, 300, and 360 cm to evaluate the system's performance in various transmission scenarios. In LOS conditions, where there is a direct path between the sender and receiver without obstacles, the SER is generally lower compared to NLOS conditions.

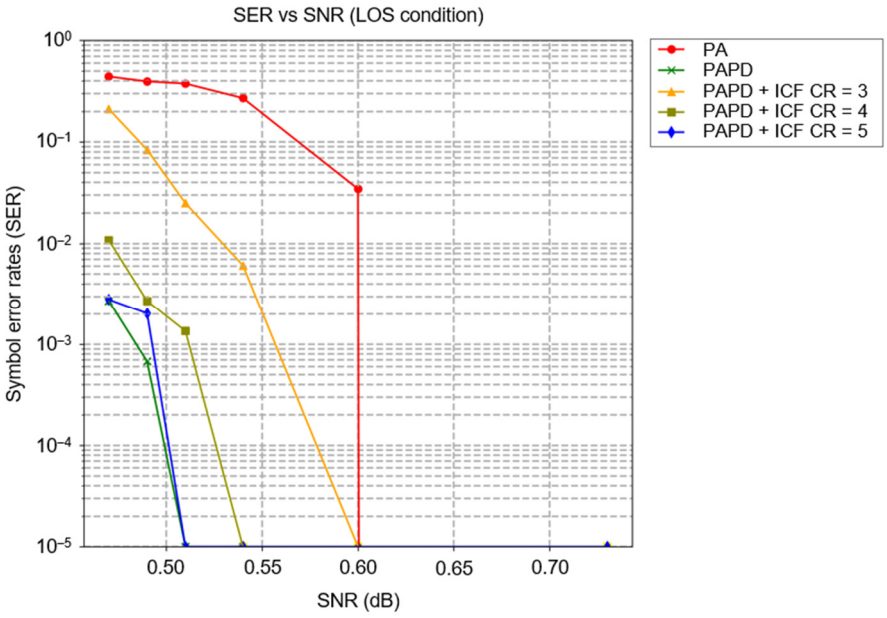

Fig. 16 The connection between distance and SER in LOS conditions

As transmission distance decreases, SER under LOS conditions decreases sharply, indicating an increase in signal strength and transmission quality. In contrast, under NLOS conditions, environmental impediments like reflection and scattering keep the SER high, especially at longer distances, and slow its drop as the distance approaches. System performance is improved

differently via different methods. PA-only systems perform the poorest with the highest SER at all distances in LOS and NLOS. PD lowered SER, especially at medium to near distances, and improved LOS performance. PA with PD employing ICF performed well in both situations, notably for CR values of 4 and 5, which consistently had the lowest SER. Environmental impediments hinder this technique's efficiency under NLOS settings compared to LOS.

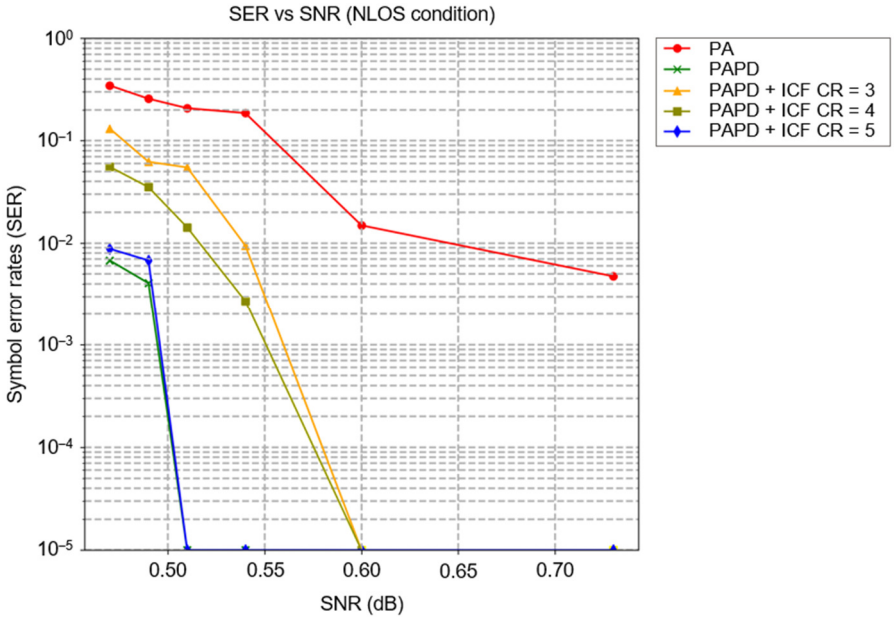

Fig. 17 The connection between distance and SER in NLOS conditions

Fig. 16 and Fig. 17 show that PD and PD with ICF applied to PA reduce SER efficiently, with better performance under LOS situations. This approach still improves wireless communication system reliability under more complex NLOS scenarios, underscoring its importance in varied transmission situations. These two methods reduce PA-induced nonlinear distortion. 5G NR and Wi-Fi 6 benefit from PAPR reduction and PA linearization. PAPR reduction reduces power peaks, improving PA efficiency, transmitter power consumption, and mobile device battery life. Hardware like PA is more durable due to lower thermal load. PA linearity upgrades reduce PA nonlinearity distortion in 5G applications, which need high frequencies and wide bandwidths for fast data speeds. PAPR reduction and PA linearization allow Wi-Fi 6 to support more uplink and downlink connections without affecting throughput or signal quality, enhancing wireless communication stability and performance.

4. Conclusion

This paper discusses two main issues in MIMO-OFDM systems: high PAPR and the nonlinear effects of PA. To mitigate these issues, the Saleh model PD technique was applied in combination with the ICF method. The proposed approach was implemented and validated in a real-world environment using SDR devices. The main conclusions are summarized as follows:

(1) The combination of the Saleh model PD and ICF effectively reduces PAPR and linearizes PA characteristics.

(2) The method enables error-free data reception and produces a clearer constellation diagram.

(3) It outperforms the PTS technique in terms of processing speed, achieving a lower execution time of 475–503 ms compared to 776 ms.

(4) The findings validate the practicality of the ICF and Saleh model integration for real-time communication systems and suggest potential applications in 5G and Wi-Fi 6 technologies.

Future work may explore hardware implementation, testing in more complex environments, and evaluation with various types of data sources.

References

[1] A. Rawat, R. Kaushik, and A. Tiwari, "An Overview of MIMO OFDM System for Wireless Communication," International Journal of Technical Research & Science, vol. VI, no. X, article no. IJTRS-V6-I10-001, 2021.

[2] M. W. Gunawan, N. A. Priambodo, M. M. Gulo, A. Arifin, Y. Moegiharto, and H. Briantoro, "Evaluations of the Predistortion Technique by Neural Network Algorithm in MIMO-OFDM System Using USRP," Jurnal INFOTEL, vol. 14, no. 4, pp. 287-293, 2022.

[3] C. Shyamala, J. Jayanth, M. Shivakumar, and A. S. Vedha, "2x2 MIMO Wireless Communication System with Alamouti Coding Using Single USRP 2944R," unpublished.

[4] M. B. Mashhadi and D. Gündüz, "Pruning the Pilots: Deep Learning-Based Pilot Design and Channel Estimation for MIMO-OFDM Systems," IEEE Transactions on Wireless Communications, vol. 20, no. 10, pp. 6315-6328, 2021.

[5] S. Elaage, A. Hmamou, M. E Ghzaoui, and N. Mrani, "PAPR Reduction Techniques Optimization-Based OFDM Signal for Wireless Communication Systems," Telematics and Informatics Reports, vol. 14, article no. 100137, 2024.

[6] M. Akurati, S. K. Pentamsetty, and S. P. Kodati, "Optimizing the Reduction of PAPR of OFDM System Using Hybrid Methods," Wireless Pers Commun, vol. 125, no. 3, pp. 2685-2703, 2022.

[7] Y. Huleihel and H. H. Permuter, "Low PAPR MIMO-OFDM Design Based on Convolutional Autoencoder," IEEE Transactions on Communications, vol. 72, no. 5, pp. 2779-2792, 2024.

[8] B. C. Agwah and M. I. Aririguzo, T Eriksson and T Svantesson, "MIMO-OFDM System in Wireless Communication: A Survey of Peak to Average Power Ratio Minimization and Research Direction," International Journal of Computer Science Engineering, vol. 9, no. 4, pp. 219-234, 2020.

[9] V. N. Tran, V. K. Vu, T. C. Nguyen, and T. H. Dang, "Optimization of Partial Transmit Sequences Scheme for PAPR Reduction of OFDM Signals," International Conference Engineering and Telecommunication, pp. 1-5, 2020.

[10] Z. Xing, K. Liu, A. S. Rajasekaran, H. Yanikomeroglu, and Y. Liu, "A Hybrid Companding and Clipping Scheme for PAPR Reduction in OFDM Systems," IEEE Access, vol. 9, pp. 61565-61576, 2021.

[11] B. Tang, K. Qin, and H. Mei, "A Hybrid Approach to Reduce the PAPR of OFDM Signals Using Clipping and Companding," IEEE Access, vol. 8, pp. 18984-18994, 2020.

[12] M. M. Gulo, I. G. P. Astawa, Arifin, Y. Moegiharto, and H. Briantoro, "The Joint Channel Coding and Pre-Distortion Technique on the USRP-Based MIMO-OFDM System," Jurnal RESTI (Rekayasa Sistem dan Teknologi Informasi), vol. 7, no. 4, pp. 930-939, 2023.

[13] S. Singhal and D. K. Sharma, "A Review and Comparative Analysis of PAPR Reduction Techniques of OFDM System," Wireless Pers Commun, vol. 135, no. 2, pp. 777-803, 2024.

[14] Z. Liu, X. Hu, W. Wang, and F. M. Ghannouchi, "A Joint PAPR Reduction and Digital Predistortion Based on Real-Valued Neural Networks for OFDM Systems," IEEE Transactions on Broadcasting, vol. 68, no. 1, pp. 223-231, 2022.

[15] V. K. Padarti and V. R. Nandhanavanam, "An Improved ASOICF Algorithm for PAPR Reduction in OFDM Systems," International Journal of Intelligent Engineering and Systems, vol. 14, no. 2, pp. 353-360, 2021.

[16] X. Liu and Q. Su, "A Comparative Study of PAPR Reduction Techniques in OFDM Systems: Simulation-Based Analysis and Performance Evaluation," IEEE 6th International Conference on Information Systems and Computer Aided Education, pp. 550-555, 2023.

[17] X. Liu, X. Zhang, L. Zhang, P. Xiao, J. Wei, and H. Zhang, "PAPR Reduction Using Iterative Clipping/Filtering and ADMM Approaches for OFDM-Based Mixed-Numerology Systems," IEEE Transactions on Wireless Communications, vol. 19, no. 4, pp. 2586-2600, 2020.

[18] S. Wang, P. Maris Ferreira, and A. Benlarbi-Delai, "Physics Informed Spiking Neural Networks: Application to Digital Predistortion for Power Amplifier Linearization," in IEEE Access, vol. 11, pp. 48441-48453, 2023.

[19] A. M. K. Bebyrahma, T. Suryani, and Suwadi, "Analysis of Combined PAPR Reduction Technique with Predistorter for OFDM System in 5G," International Seminar on Intelligent Technology and Its Applications, pp. 478-483, 2022.

[20] S. G. Shivaprasad Yadav and Meghana, B. R, and B. R, "Digital Predistortion (Dpd) Algorithm for 5G Applications," Natural Volatiles & Essential Oils, vol. 8, no. 6, pp. 888-904, 2021.

[21] H. Al-kanan, X. Yang, and F. Li, "Improved Estimation for Saleh Model and Predistortion of Power Amplifiers Using 1-dB Compression Point," The Journal of Engineering, vol. 2020, no. 1, pp. 13-18, 2020.

[22] M. Beikmirza, L. C. N. de Vreede, and M. S. Alavi, "A Low-Complexity Digital Predistortion Technique for Digital I/Q Transmitters," IEEE/MTT-S International Microwave Symposium - IMS 2023, pp. 787-790, 2023.

[23] L. Chandini and A. Rajagopal, "PAPR Reduction in SDR-Based OFDM System," Evolutionary Computing and Mobile Sustainable Networks: Proceedings of ICECMSN 2021, pp. 1051-1065, 2021.

[24] Y. Liu, H. Song, H. Wen, Z. Yu, and W. Li, "Performance Evaluation of the MIMO-OFDM System Using Artificial Noise Based on the SDR Platform," 2023 2nd International Conference on Computing, Communication, Perception and Quantum Technology, pp. 130-135, 2023.

[25] G. M. Abdulsahib, D. S. Selvaraj, A. Manikandan, S. Palanisamy, M. Uddin, O. I. Khalaf, et al., "Reverse Polarity Optical Orthogonal Frequency Division Multiplexing for High-Speed Visible Light Communications System," Egyptian Informatics Journal, vol. 24, no. 4, article no. 100407, 2023